JOURNAL OF COMPUTATIONAL PHYSICS 24, 108–114 (1977)

Note

Three-Dimensional Low Reynolds Number Flows with a Free Surface

DAVID DEGANI

Computational Fluid Dynamics, NASA Ames Research Center, Moffett Field, California 94036

AND

CHAIM GUTFINGER

Department of Mechanical Engineering, Carnegie–Mellon University, Pittsburgh, Pennsylvania 15213

Received July 13, 1976; revised October 19, 1976

INTRODUCTION

Only a few numerical techniques for three-dimensional incompressible transient flow calculations have been published [1]. All these techniques are not suitable for cases where the Reynolds numbers of the flows are small and the no-slip boundary condition on the rigid wall and the boundary condition on the free surface are not negligible. In that case one has to solve the flow equations by means of an iterative scheme, as was done in the two-dimensional case [2, 3]. The solution here is an extension of the two-dimensional leveling problem [3] to the 3-D case when the Re of the flow is very low and the free surface boundary condition including surface tension effects is taken into account. Several examples of the calculation are presented with comparisons to experimental results and the two-dimensional numerical solution.

BASIC EQUATIONS AND METHOD OF SOLUTION

The numerical solution is based on the Marker and Cell (MAC) method [4] when the calculational region is divided into a finite number of stationary rectangular cells (boxes in the 3-D case) and the fluid flows through them.

The velocity components $\bar{V}(u, v, w)$ are given on the surface of the box and the pressure ϕ in its center (Fig. 1). The fluid behavior and the free surface shape is computed using finite difference approximations for the conservation form of Navier–Stokes equations and the conservation of mass equation:

$$D\bar{V}/Dt = -\nabla\phi + \nu\nabla^2\bar{V} + \bar{g}, \tag{1}$$

$$\nabla \cdot \bar{V} = 0. \tag{2}$$

ISSN 0021-9991

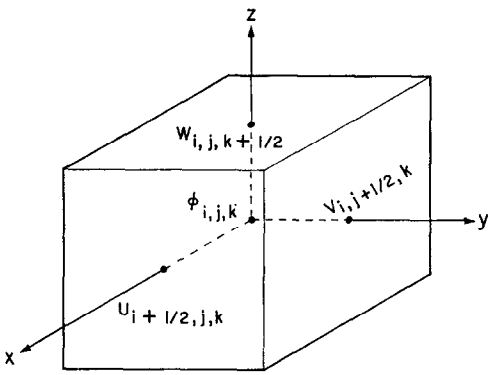

FIG. 1. Position of field variables on mesh.

A Poisson equation for pressure is obtained by differentiation and addition of (1)

$$\nabla^2\phi = -R \tag{3}$$

where R is

$$R \equiv (u^2)_{xx} + (v^2)_{yy} + (w^2)_{zz} + 2[(uv)_{xy} + (uw)_{xz} + (vw)_{yz}] + D_t - \nu\nabla^2 D,$$

$$D \equiv u_x + v_y + w_z .$$

Boundary Conditions

On the rigid wall the no-slip condition is satisfied for the velocity, while the pressure boundary condition one can get from the momentum equations. If the curvature of the free surface is small, we can approximate the normal and tangential stress conditions by the expressions:

$$\phi - 2\nu\, \partial u_n/\partial n = 0, \tag{4}$$

$$\nu(\partial u_n/\partial s + \partial u_s/\partial n) = 0, \tag{5}$$

where n, s are the outward normal and tangential directions, respectively.

In order to reduce the computation time the boundary conditions at the free surface are calculated only for the special case of three orientations of the free surface cells, as seen in Fig. 2 (this assumption is sufficient for a case of standing waves, like in the case of leveling problems depicted in Fig. 3). For example, the cells in Fig. 2a are surface cells, the adjacent cells in the z direction are empty, and adjacent cells in the $(-z)$ direction are full or surface cells. For all the three cases we have to calculate the normal stress at cell (i, j, k) according to Eq. (4) and two tangential stresses perpendicular to each other using Eq. (5).

In order to reduce the computation time required to find the position and orientation of the surface cell, 18 different kinds of cells were defined according to the boundary conditions to be calculated in the particular cell (instead of four kinds of cells in the MAC method).

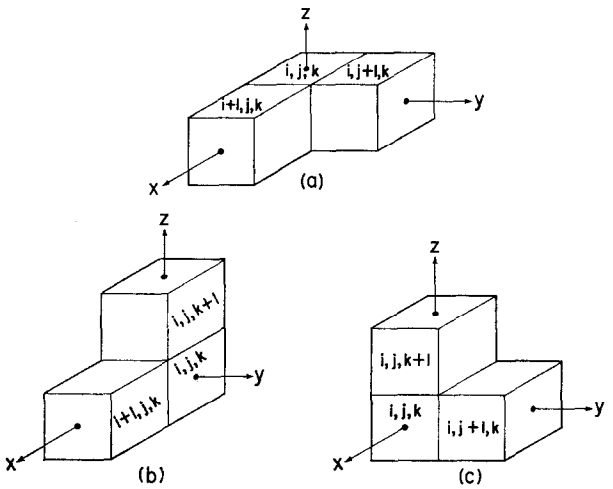

FIG. 2. Surfaces for determination of normal and tangential stresses: (a) horizontal, (b) vertical surface in y-direction, (c) vertical surface in x direction.

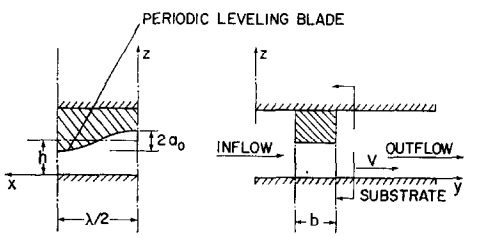

FIG. 3. Three-dimensional computational field.

For low Reynolds number the diffusion terms are dominant with respect to the convection terms, therefore we expressed the convection terms and R (from Eq. (3)) at time $n\,\Delta t$.

The four linearized equations (for u, v, w, and ϕ) were solved simultaneously by an iteration technique together with the free surface boundary conditions at time $(n+1)\,\Delta t$. Using the new velocities the new shape of the free surface and the surface tension force were calculated for the next time step.

In the first stage of the work [5] the S.O.R. method was used to solve the coupled equations. A typical problem of $10 \times 20 \times 24$ cells needed 312K core memory (on IBM 370/168) and 30–50 iterations per time step (0.54 sec per iteration). This method, although efficient enough for the 2-D case [3], was found inefficient in the 3-D case. By using a variant of the Alternating Direction Method analyzed by Samarskii [6] and Chorin [7], the computation time was reduced about 40%. Another possibility to reduce the computation time is to extend the ADI Douglas–Rachford method, analyzed by Deville [8] for the 2-D case, to the 3-D case.

Free Surface and Surface Tension Calculations

In order to impose this boundary condition, it is necessary to know the position and the orientation of the free surface cells. Instead of using particles for finding the free surface cells (MAC method), the method of Nichols and Hirt [1] was extended for this purpose.

The kinematic condition for the free surface $\eta(x, y, t)$ is given by

$$w = D\eta/Dt. \tag{6}$$

Thus, we can calculate η from the values of the velocities on the free surface. We place imaginary rods, the height of each rod marking the height of the free surface $\eta(x, y, t)$ at that point. The spacings between the rods being determined by the accuracy requirements of the surface tension computation. The height of the rods changes with time according to Eq. (6) (and it is solved by a method suggested by Hirt [9]). The velocity components at the surface points corresponding to the rod's tips are computed by means of a second-order Taylor expansion, using the velocity field at time $(n + 1)\,\Delta t$.

The surface tension was introduced into the momentum equations as a body force [10]. The surface tension was computed in planes parallel to the x–z plane only (Fig. 3), and perpendicular to x–y plane, assuming the radius of curvature in (y–z) planes to be large.

The tips of the rods describing the free surface were fitted with a cubic curve using the spline fit method. The first and second derivatives of the curve were computed for the center of each cell and the components of the surface tension force were calculated, using these derivatives, and introduced into the respective momentum equations.

Computational Results

Using the technique described above, several cases of the 3-D leveling problem were computed. According to Fig. 3 a static leveling blade with a periodically vary edge was held in place at distance $z = h$ from the substrate ($z = 0$) which was moving in the positive direction of the y axis with a constant velocity V. The fluid was being introduced into the computational field (inflow) and removed from the field (outflow) at a uniform velocity V. In order to simplify the problem and to allow approaching steady state solution the excess fluid from the left edge of the blade was removed artificially. Figures 4 and 5 are plotter output of steady state solutions for two different leveling blade widths (b in Fig. 3).

Figures 6 and 7 are comparisons between experimental results from Degani and Gutfinger [3, 11], the 3-D computational results, and 2-D results from [3]. One can see that the 2-D solution is good enough in cases when b/h is small, while for other cases the three-dimensional approach should be chosen.

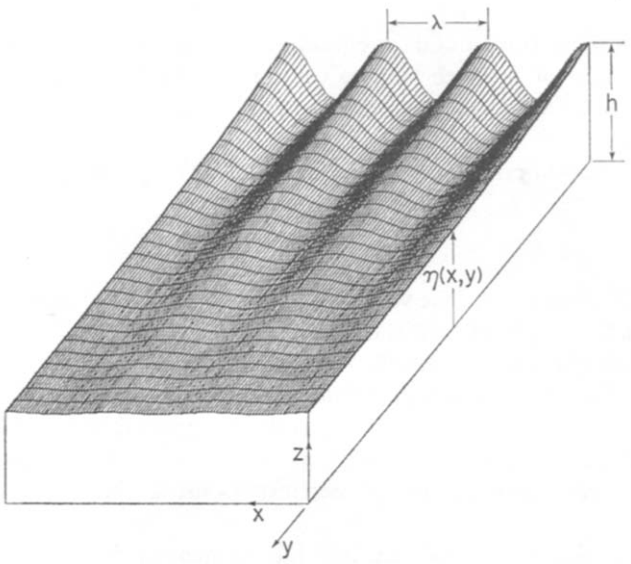

FIG. 4. Plotter output for 3-D leveling problem. ($b/h = 1$, $V = 10$ cm/s, $\sigma = 70$ d/cm, $\nu = 120$ cm^2/s, $\rho = 1.5$ g/cm^3).

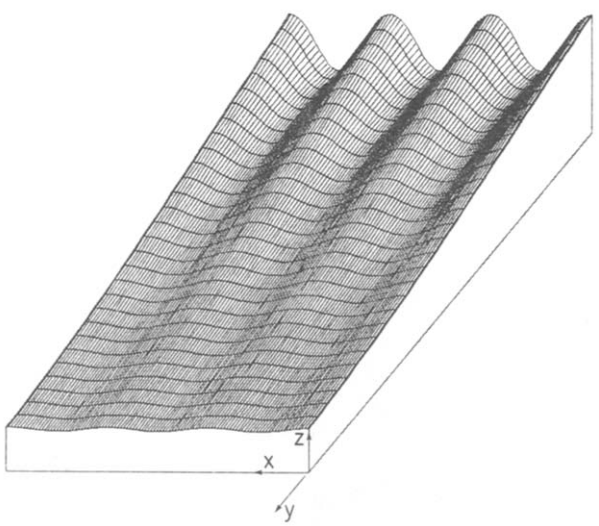

FIG. 5. Plotter output for 3-D leveling problem. ($b/h = 20$, $V = 10$ cm/s, $\sigma = 70$ d/cm, $\nu = 120$ cm^2/s, $\rho = 1.5$ g/cm^3).

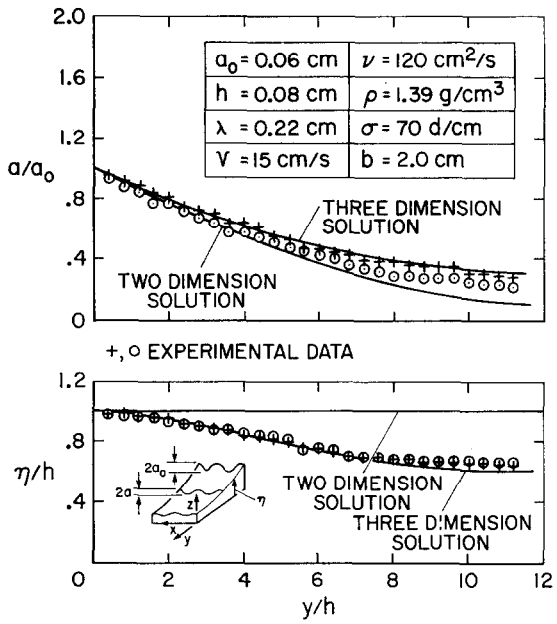

FIG. 6. Amplitude, a, and film thickness, η, vs y. $b/h = 25$.

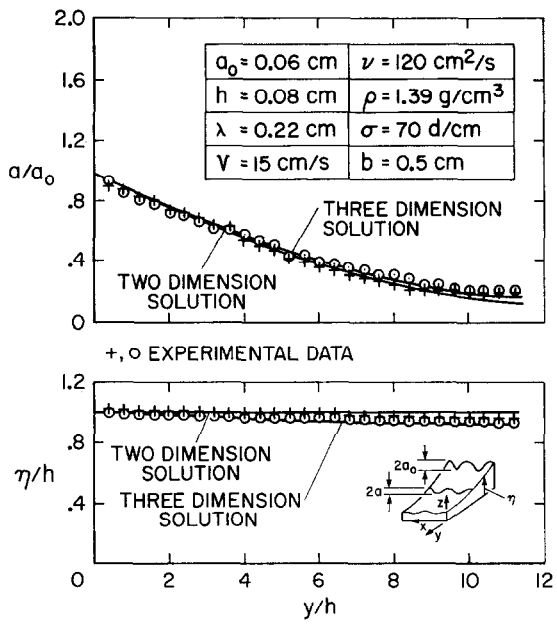

FIG. 7. Amplitude, a, and film thickness, η, vs y. $b/h = 6.2$.

REFERENCES

1. B. D. NICHOLS AND C. W. HIRT, *J. Computational Phys.* **12** (1973), 234.
2. W. E. PRACHT, *J. Computational Phys.* **7** (1971), 46.
3. D. DEGANI AND C. GUTFINGER, "Computers and Fluids," 1976, in press.
4. F. H. HARLOW AND J. E. WELCH, *Phys. Fluids* **8** (1965), 2182.
5. D. DEGANI, Ph.D. Dissertation, Technion, Israel Institute of Technology, Haifa, Israel, 1975.
6. A. A. SAMARSKII, *U.S.S.R. Comput. Math. and Math. Phys.* **2** (1962), 894.
7. A. J. CHORIN, *Math. Comput.* **22** (1968), 745.
8. M. O. DEVILLE, to be published in *J. Méchanique*, Belgium.
9. C. W. HIRT, *J. Computational Phys.* **2** (1968), 339.
10. B. J. DALY, *J. Computational Phys.* **4** (1969), 97.
11. D. DEGANI AND C. GUTFINGER, *Israel J. Technol.* **12** (1974), 191.